RSC Advances

ROYAL SOCIETY OF CHEMISTRY

www.rsc.org/advances

Dye-collagen interactions. Mechanism, kinetic and thermodynamic analysis.

Maria Victoria Tuttolomondo[1], Juan Manuel Galdopórpora[1], Lea Trichet[2], Hugo Voisin,[2] Thibaud Coradin[2], Martin Federico Desimone[1*]

[1]IQUIMEFA-CONICET. Facultad de Farmacia y Bioquimica, Universidad de Buenos, Aires, Junin 956 Piso 3., (1113) Ciudad Autónoma de Buenos Aires, Argentina.

[2]Sorbonne Universités, UPMC Univ Paris 06, CNRS, UMR 7574, Laboratoire de Chimie de la Matière Condensée de Paris, F-75005 Paris, France;

*E-mail: desimone@ffyb.uba.ar; Fax: +54-1149648254; Tel: +54-1149648254

In memoriam Prof. Dr. Luis E. Diaz.

Abstract

A large family of azo dyes have been developed and used in the textile industry, including for leather tainting, and are therefore expected to exhibit strong interactions with collagen-based materials. Here we investigate the mechanisms of adsorption of the Remazol black B dye on type I collagen hydrogel. Higher and stronger retention of the dye is achieved in alkaline conditions, correlated with enhanced thermal and mechanical stability of the hydrogel. The formation of a covalent bond between the dye and the protein network via Michael reaction is suggested and supported by the detailed analysis of the kinetics and thermodynamics of the sorption reaction. Type I collagen hydrogels combine low cost, fast sorption, high loading and strong retention capacity together with low storage volume, making them promising materials for dye remediation. Dye-modified hydrogels may also find applications in the biomedical field.

1. Introduction

The use of dyes is a widespread practice employed to change the characteristics of substances as different as fabric, paper, leather, foodstuff and drugs among many others. In the beginning dyes were obtained from natural sources like plants and animals. At the early stages of the XXth century these practices were abandoned and synthetic dyes were used instead. The greatest consumer of dyestuff is the textile industry with roughly 60% of the total amount of dyes. The rest is divided among leather dying industry, paper production, color photography, pharmaceuticals and medicine, cosmetics, wood dying, agriculture, investigation, biology and chemistry, photoelectric cells, etc. [1, 2] Dyes can be classified according to their color index or can be grouped in different classes according to their application and chemical behavior: acid, basic, direct, disperse, metallic, mordant, pigments, and reactive dyes. Reactive dyes have a relatively simple structure and are chemically composed by azo compounds, anthraquinones and phtalocyanines. The absolute majority of the synthetic dyes used are azo dyes. [3]

From an environmental point of view, special interest in dyes arises from the fact that, even at very low concentration (down to 1 ppm), they can make water highly colored, making it not only aesthetically unacceptable, but also preventing light from reaching the deeper layers of water curses, altering the flora and in consequence the fauna of the aqueous ecosystems. There are cases where this change is so drastic that eutrophication takes place.[4] In addition, azo dyes (whatever their type) can suffer N=N bond rupture if the conditions of the medium are reductive, producing and releasing aromatic amines to the water bodies. These amines are considered extremely toxic due to their carcinogenic properties. [5-7]

Traditional waste water treatments are generally inefficient when dealing with water contaminated with such kinds of synthetic dyes because of their chemical stability. [8] There

are many ways of treating contaminated waters, namely physical, chemical and biological treatments. [9-14] The less costly are the physical ones based on adsorption. [15-18] When dealing with azo dyes the latter can be considered the safest because no breakage of the azo bond occurs, drastically diminishing the probability of generating potentially toxic aromatic amines.[19] On the other hand, a common problem associated with adsorption is related to the adsorption products disposal, which implies a waste moving cost to a preliminary storage place before the final disposal of the waste. Additionally, this transient storage place can create a second contamination source if the dye leaks out or permeates through the sorbent and reaches the soil.

Considering that many dyes have been developed for strong binding on leather products that are skin-based materials and, therefore, rich in type I collagen, we hypothesized that collagen hydrogels could also interact strongly with these molecules. Type I collagen is a very abundant and well characterized biomolecule that accounts for 35% of the dry weight of any mammal. The basic structure of type I collagen is –gly-X-Y-gly- where X and Y are proline and 4-hydroxyproline respectively. [20-24] From a physicochemical point of view it is a semi-flexible helicoidal polyelectrolyte, 300 nm in length and 1.5 nm in diameter. Assembled within fibrils, the collagen molecule ends are displaced from each other about 67 nm, which produces the characteristic striations seen in TEM microscopy. Importantly type I collagen is a waste product of many industries and it is cheap and easy to obtain in a purified form. [25]

In this work, we have studied the adsorption of Remazol black B, a sulfonated reactive azo dye, on type I collagen hydrogels. We demonstrate that the highest sorption rates are obtained in alkaline conditions where electrostatic interactions are expected to be repulsive, suggesting the formation of covalent bonds between the dye and the protein network via a

Michael addition reaction. This hypothesis is supported by the significant increase in thermal stability and rheological properties of the hydrogels. Detailed kinetics and thermodynamic analyses enlighten the co-existence of weak and strong chemisorption processes, whose balance depends on pH and dye concentration. Altogether type I collagen hydrogels combine several chemical, physical and economical advantages for their application as water cleaning sorbents. Further investigation of the biological behavior of dyed hydrogels will also be of interest.

2. Experimental

2.1. Collagen extraction and hydrogel preparation

Type I collagen was purified from rat tails. Tails were washed with a solution of acetone/ethanol. Collagen was extracted by breaking the distal extreme of the tail, cutting the soft tissue and extracting the tendon. This action was repeated until there was no tendon left. Tendons were stocked in a sterile saline solution and washed with saline solution 3 times to clean the blood in them. When the supernatant was clean, tendons were washed with a sterile 4M NaCl solution for red cell lysis and were then dissolved in sterile 500 mM acetic acid while stirring at 4°C overnight. A differential precipitation of type I collagen was performed with a 700 mM NaCl solution. Once collagen has precipitated, the supernatant was discarded and the precipitate put back in sterile 500 mM acetic acid solution and left to dissolve overnight. [21, 25-28] The following day, aliquots were taken for quantification using the hydroxyproline method. [29]

After adjustment of the collagen concentration to 1.75 mg mL^{-1} with 500 mM acetic acid, aliquots of 250 µl of the solution were put in each well of a 24-well plate. The plate was

incubated in NH$_3$-saturated atmosphere at 20°C until the hydrogel was obtained. The hydrogels were then left in a fume hood to evaporate the ammonia until the pH was neutral.

2.2. Materials characterization

Samples for scanning electron microscopy (SEM) were fixed using 3.63% glutaraldehyde in 50 mM sodium cacodylate buffer (pH 7.40) with 300 mM saccharose for 1 h at 4°C. Following fixation, samples were washed three times in the same buffer and then dehydrated in a graded series of ethanol (70%, 95% and two changes of alcohol 100%). Finally, the samples were subjected to CO$_2$ supercritical drying. Recovered samples were gold sputter-coated for observation with a Zeiss SUPRA 40 microscope. For transmission electron microscopy (TEM), following fixation and washing steps described above, the samples were post-fixated using 2% osmium tetraoxide in 50 mM sodium cacodylate buffer (pH 7.40) with 300 mM saccharose for 1 h at 4°C. Samples were then washed three times in the same buffer, dehydrated with ethanol and embedded in araldite. Thin araldite transverse sections (70–80 nm) were made with an Ultracut ultramicrotome and contrasted by phosphotungstic acid. Recovered sections were imaged using a Zeiss 109 microscope.

Differential Scanning Calorimetry (DSC) measurements were performed on a TA instrument model Q20. Temperature was calibrated with In (430 K, 3.3 J.mol^{-1}). Approximately 20 mg of each sample was first equilibrated at 20°C before a ramp of temperature of 5°C.min^{-1} up to 90°C was applied.

Rheological measurements were conducted on an Anton-Paar rheometer model MCR 302. The geometry used was a 25 mm diameter disk with a rough surface (reference PP 25/S). Collagen hydrogel at a 1.75 mg.mL^{-1} concentration were placed in PTFE circular chambers with an inner diameter slightly larger than the geometry allowing rheological measurements

at low modulus range. These samples were incubated in NH_3 saturated atmosphere at 20°C overnight and then washed with water and Tris buffer pH 9.00. The obtained hydrogels were incubated for 2 days either with an aqueous solution (8 mL) of Remazol Black 2 mg.mL^{-1} in Tris buffer or with Tris buffer alone for controls. The rheological behavior of the samples was investigated under sinusoidal deformations with a frequency of oscillations ranging from 0.1 to 100 Hz at set strain (0.1 %) and under a normal force of 0.04 N. Frequency dependence of G' and G" was recorded and oscillations up to 10 Hz were considered consistent. All experiments and their corresponding measurements were conducted in triplicate.

The FTIR spectra of samples were recorded on a Bruker spectrometer model Equinox 500. The hydrogels were lyophilized overnight and then crushed in a powder. The powder was then disposed on the diamond crystal of a Universal ATR Sampling Accessory and pressed before the obtention of the spectrum between 4000 and 600 cm^{-1} with a resolution of 1 cm^{-1}. 16 scans were recorded under dry air purge. The corresponding measurements were conducted in triplicate. As a control a spectrum of Remazol black powder was also recorded.

The hydrogels used to perform rheology analysis were lyophilized overnight and then crushed as a powder. The powder was then disposed on the crystal of a Universal ATR Sampling Accessory and pressed before recording the spectrum between 4000 and 600 cm^{-1}. The corresponding measurements were conducted in triplicate. As a control a spectrum of Remazol black powder was also recorded.

2.3. Remazol black B adsorption studies

Adsorption experiments were carried out by a batch method at room temperature (25 ºC) with constant stirring (120 rpm). A fixed aliquot of the collagen hydrogels (250 µl of a 1.75 mg.mL^{-1}) was incubated with an aqueous solution (1 mL) of the azo dye, with concentrations ranging from 5 µg.mL^{-1} to 800 µg.mL^{-1}. The effect of pH, interaction time and dye concentration on its sorption were determined by monitoring the absorbance of the supernatant at 595 nm using an UV–Vis Spectrophotometer (Cecil CE 3021, Cambridge, England).

In additional experiments, Remazol black solutions were subjected to two pretreatments. In first place, an 800 µg.mL^{-1} sodium bisulphite solution was added to a 2 mg.mL^{-1} dye solution and the reaction left to proceed for 30 minutes at 60 °C to inactivate the vinylsulphone. [30] Alternatively, hydrolysis of the vinylsulphone group of the dye was achieved by reaction with a 10 mg.mL^{-1} NaOH solution at 90°C for 1 hour, according to the procedure described by Agarwal *et al*. [30]

All experiments and their corresponding measurements were conducted in triplicate under identical conditions and statistically analyzed by one-way ANOVA. In all cases, the differences were considered to be significant when $p < 0.05$.

2.4 Kinetics and thermodynamic modeling

In order to analyze the adsorption rates kinetic analysis using the pseudo-first-order, pseudo-second-order, Elovich and the modified Freundlich equations were performed.

The pseudo-first-order equation is the simplest and most used to describe the adsorption of a solute in liquid solution onto an adsorbent. The law that defines the first order equation is:

$$\frac{dq_t}{dt} = k_1(q_e - q_t) \qquad\qquad\qquad (1)$$

where k_1 is the pseudo first order adsorption constant (min^{-1}), q_e and q_t (μg.mg^{-1}) denote the amount of adsorbed dye at equilibrium and at time t (min) respectively. Equation 1 can be integrated to get:

$$q_t = q_e(1 - e^{-k_l t}) \qquad\qquad\qquad (2)$$

Values of k_l and q_e were evaluated by nonlinear regression of the q_t *vs.* t curves. Alternatively, dye adsorption onto porous materials can follow a pseudo-second-order law that assumes the existence of delay in the adsorption process due to the presence of an outer limit layer or an external resistance. It can be expressed in the following way:

$$\frac{dq_t}{dt} = k_2(q_e - q_t)^2 \qquad\qquad\qquad (3)$$

where k_2 (mg.μg^{-1}.min^{-1}) is the pseudo second order constant. When integrated, this equation leads to:

$$q_t = \frac{(k_2 q_e^2 t)}{(1 + k_2 q_e t)} \qquad\qquad\qquad (4)$$

values of k_2 and q_e were evaluated by nonlinear regression of the q_t *vs.* t curve.

The Elovich equation can be applied to chemisorption processes and assumes that the adsorption sites are heterogeneous. It can be expressed as

$$q_t = \frac{1}{\beta \ln[1+(\alpha\beta t)]} \qquad (5)$$

where the constant α (mg.g^{-1}.h^{-1}) is the initial adsorption rate and β (g.mg^{-1}) is related to the amount of surface covered and the activation energy involved in the chemisorption process.

The modified Freundlich model, first developed by Kuo and Lotse, is described by

$$q_t = k_F C_0 t^{\frac{1}{m}} \qquad (6)$$

where k_F (L.g^{-1}.h^{-1}) is the apparent adsorption constant, C_0 (mg.L^{-1}) is the initial sorbate concentration and m (adimensional) is the Kou-Lotse constant. This model can describe diffusion processes controlled by surface; in particular, it can describe kinetics controlled by intra particle diffusion when m tends to 2. [31]

2.5 Adsorption isotherms

The maximum adsorption capacity of the hydrogels Q (μg.mg^{-1}) was determined after 24 h of contact with the dye solution using the following equation:

$$Q = \frac{(C_i - C_e)}{Vm} \qquad (7)$$

9

Where C_i and C_e are the initial and equilibrium dye concentrations in µg.mL^{-1}, V is the

tested solution volume (mL) and m (mg) is the collagen mass in the hydrogel. [26, 27]

Langmuir and Freundlich models have been widely used to fit data in the biosorption

equilibrium process. The first of them hypothesizes that the interaction between sorbate and

sorbent is homogeneous, with homogeneous union sites until the first monolayer is formed

on the sorbent surface. The second model has a better fit when adsorption sites are

heterogeneous and have different interactions.[32] The equations that describe both isotherms

are:

Langmuir:

$$q_{eq} = \frac{q_m K_a C_{eq}}{1 + K_a C_{eq}} \qquad (8)$$

Freundlich

$$q_{eq} = k C_{eq}^n \qquad (9)$$

where C_{eq} is the dye concentration in the equilibrium, K_a is the equilibrium constant, q_m is

the maximum adsorption capacity (µmol.g^{-1}) and k are n are arbitrary parameters.

Another equation that was initially applied to gases but can be used to fit biosorbent

adsorption data is the Dubinin-Radushkevich (DR) equation. This model assumes that

pores are filled with adsorbed molecules according to adsorption force fields in the

micropores and the interactions with the adsorbed molecules. When applying this equation

to adsorption on solid phase, the adsorbed amount at any sorbate concentration is assumed to be a gaussian function of the Polanyi potential (ε): [33]

$$q_{eq} = q_{DR}e^{-k_{DR}\varepsilon^2} \tag{10}$$

where

$$\varepsilon = RT \ \ln\left(1 + \frac{1}{C_{eq}}\right) \tag{11}$$

Where q_{DR} is the maximum capacity, k_{DR} (mol^2.kJ^{-2}) is a constant related to the adsorption energy and C_{eq} (g.g^{-1}) is the concentration at equilibrium.

The Temkin isotherm includes a factor that explicitly considers the sorbate-sorbent interactions. If extremely low and high values are ignored, the model assumes that the sorption heat (that is a function of the temperature) of all the molecules of a layer will decrease linearly instead of logarithmically as each layer is completed. [34]

$$q_e = \frac{RT}{b_T \ln(A_T C_e)} \tag{12}$$

$$B = \frac{RT}{b_T} \tag{13}$$

$$q_e = B \ln A_T + B \ln C_e \tag{14}$$

Where A_T is the Temkin equilibrium constant (L.g^{-1}), b_T is the Temkin constant, R is the universal gas constant (8.314 J.mol^{-1}.K^{-1}), T is the temperature (K) and B is a parameter related to the heat of sorption (J.mol^{-1}).

3. Results and discussion

Figure 1a shows a representative SEM image of the prepared collagen hydrogel. It consists of a fibrous network (with fibers *ca*. 60 nm in diameter) exhibiting a high porosity level, with an average pore size larger than 200 nm, characteristic of these hydrogel structures. This image confirms that the self-assembly of the collagen molecules to create the collagen fibrils was successful achieved. SEM images at higher magnification revealed the periodic banding pattern of the collagen fibrils, a typical feature of the physiological structure of type I collagen (**figure 1b**). The characteristic transversal cross-striations with a periodicity of 67 nm were more clearly evidenced on TEM images (**figure 1c**).
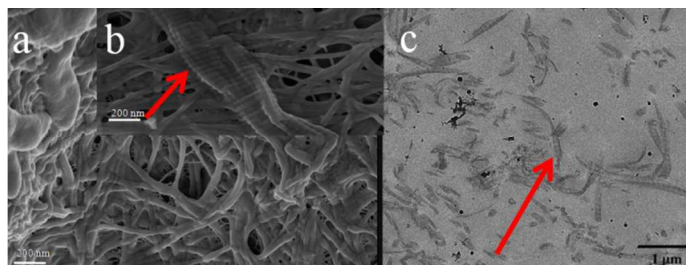
Figure 1: (a) SEM image showing the microstructure of the collagen hydrogel; (b) Insert with detail of the striations; (c) TEM image of the collagen hydrogel where the characteristic banded pattern of the collagen fibrils can be evidenced.

The adsorption of Remazol Black on these collagen hydrogels was investigated at pH 5.00, 7.00 and 9.00. As can be seen in **figure 2**, no significant difference in adsorption rate ($p <$ 0.05) was evidenced when sorption was performed at pH 5.00 and 7.00, where 60 % of the initial dye content is adsorbed. In contrast, at pH 9.00, nearly 80 % of the dye was adsorbed to the collagen hydrogel.
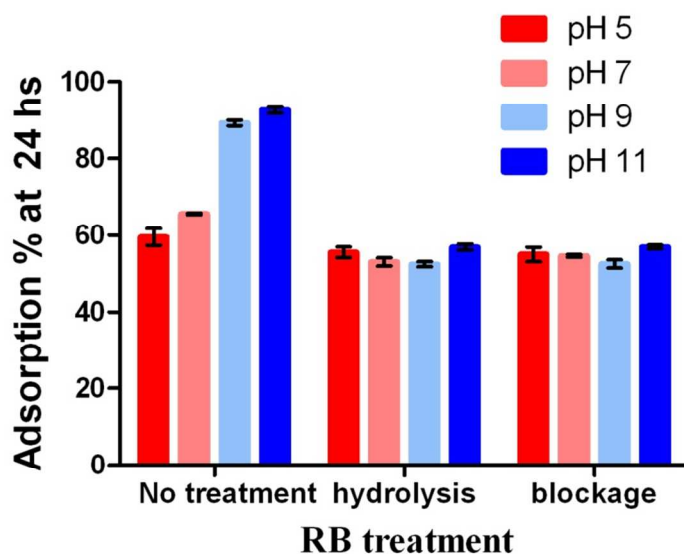
Figure 2: Influence of pH and dye chemical modification on the adsorption rate (%) of Remazol Black onto collagen hydrogel after 24 h. The initial concentration of RB was 100 μg.mL^{-1}. Results are presented as the mean± SD of triplicate experiments. *shows statistically significant difference $p<0,005$

Type I collagen is a polyampholyte polymer with 15-20 % ionizable charges. Its maximum positive charge is achieved at pH 2.50 (+ 254 mV) and its isoelectric point is *ca*. pH 9.20. Between pH 6.50 and 9.00 it shows minimal electrostatic repulsion with a net value of + 38

mV. [20] Thus at pH of 5.00 and 7.00, collagen matrices are slightly positively-charged due to the presence of protonated amines allowing for attractive electrostatic interaction with the sulfonate-bearing negatively-charged RB molecules.[35, 36] However, these electrostatic interactions cannot account for the increase in dye sorption observed at pH 9.00. Rather it can be attributed to another reaction following the Michael addition mechanism that was previously reported to occur between vinylsulfone-bearing reactive dyes and free –NH$_2$ (or –OH) groups of proteins, such as keratin and silk, in alkaline media. [30, 37-41] This reaction proceeds following the scheme presented in **figure 3**.
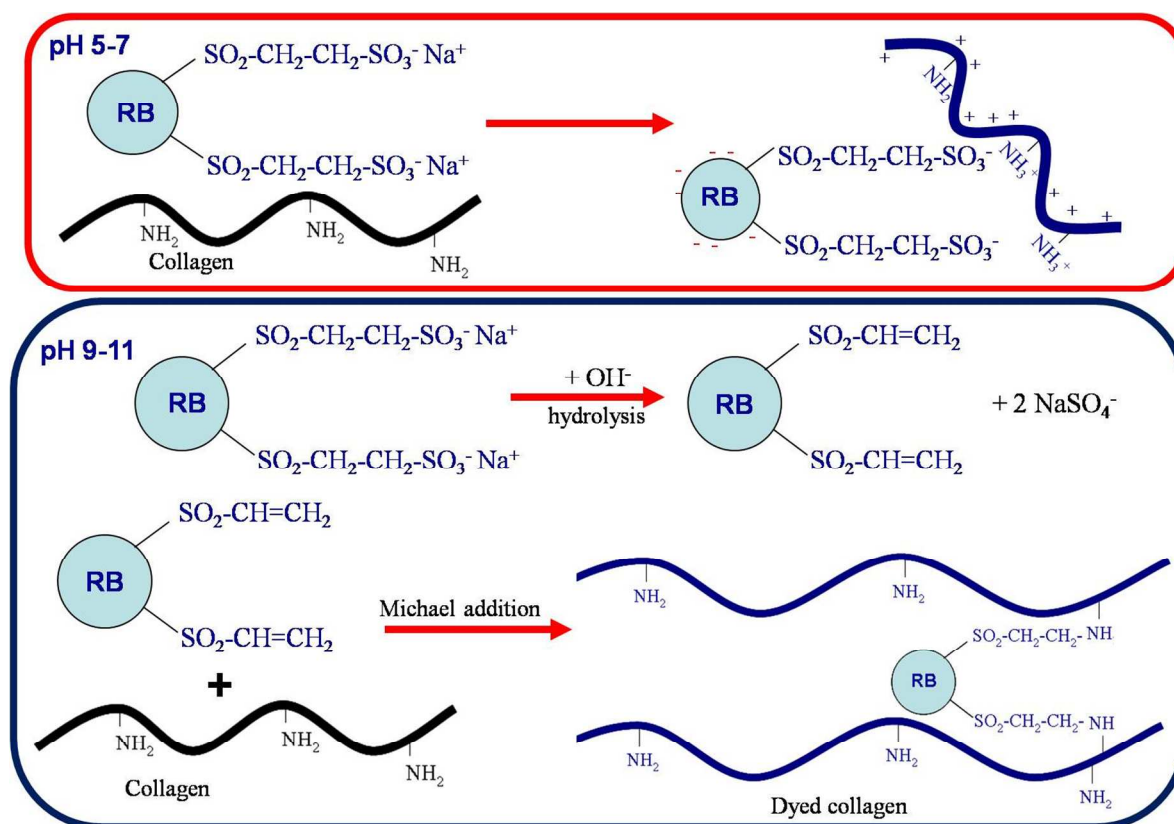
Figure 3: Scheme of the Michael reaction between Remazol Black and collagen hydrogels.

To test this hypothesis, the dye molecule was submitted to two different treatments, *i.e.* hydrolysis and blockage of the sulfonate group, before being put in contact with the collagen hydrogel. As shown on **Figure 2** both treatments leveled down the adsorption rates, which became insensitive to pH, supporting the idea that the vinylsulfone groups are involved in the non-electrostatic interactions occurring at pH 9.00 between the plain dye and collagen. Noticeably, the collagen molecule has a relatively small amount of free amino (lysine, arginine, histidine: 8 %) and hydroxyl groups (serine, hydroxyproline, threonine: 14 %) capable of reacting with the vinylsulphone group of the reactive dye *via* the Michael addition pathway, in fair agreement with the 20 % increase in dye removal at pH 9.00 compared to neutral and acidic conditions.

Attempts made to desorb the dye at various pHs (from 4 to 10) and temperatures (from 4°C to 37°C) or using urea 6 M and NaCl 6M were unsuccessful. Competitive sorption assays using other molecules with sulfate moieties such as chondroitin sulfate or the sodium sulfate salt did not hinder the binding of the dye. These results further support the existence of a covalent interaction between the dye and the collagen gel.

Attempts were made to identify the formation of the dye-collagen bond at pH 9.00 using FTIR. The main absorption bands in collagen samples are those from amide A (3400–3440 cm^{-1}), amide I (C=O stretching, 1656 cm^{-1}), amide II (N−H stretching, 1592 cm^{-1}) and amide III (C−N stretching and N−H stretching, 1145-1300 cm^{-1}). These peaks validate the integrity in the conformation of the collagen molecules. Additional peaks at 1450 cm^{-1}, 1315 cm^{-1} and 1240 cm^{-1} are associated with C−H bending modes $C(CH_2)_2$ torsion and CN stretching/ NH deformation, respectively. The ratio of transmission intensity T_{1454}/T_{1234} often used to assess the stability of proteins is close to 1, which indicates that the triple helical structure of collagen is conserved. [42]

Remazol Black B displays peaks at 3483, 2929, 1660 and 1490 cm^{-1}, for –OH stretching vibration, aromatic -CH stretching vibration, -C=C- stretching and -N=N- stretching vibration, respectively. [43] Peaks at 1053 cm^{-1} and 1124 cm^{-1} represent the SOO asymmetric stretching in sulfonic acid groups. These peak values confirm the presence of $–SO_3^-Na^+$ moieties in the dye structure. [43] As shown on **Figure 4**, the FTIR spectra of the dyed hydrogel gathers the main vibration bands of the two components, without significant variations in the relative peak intensities.
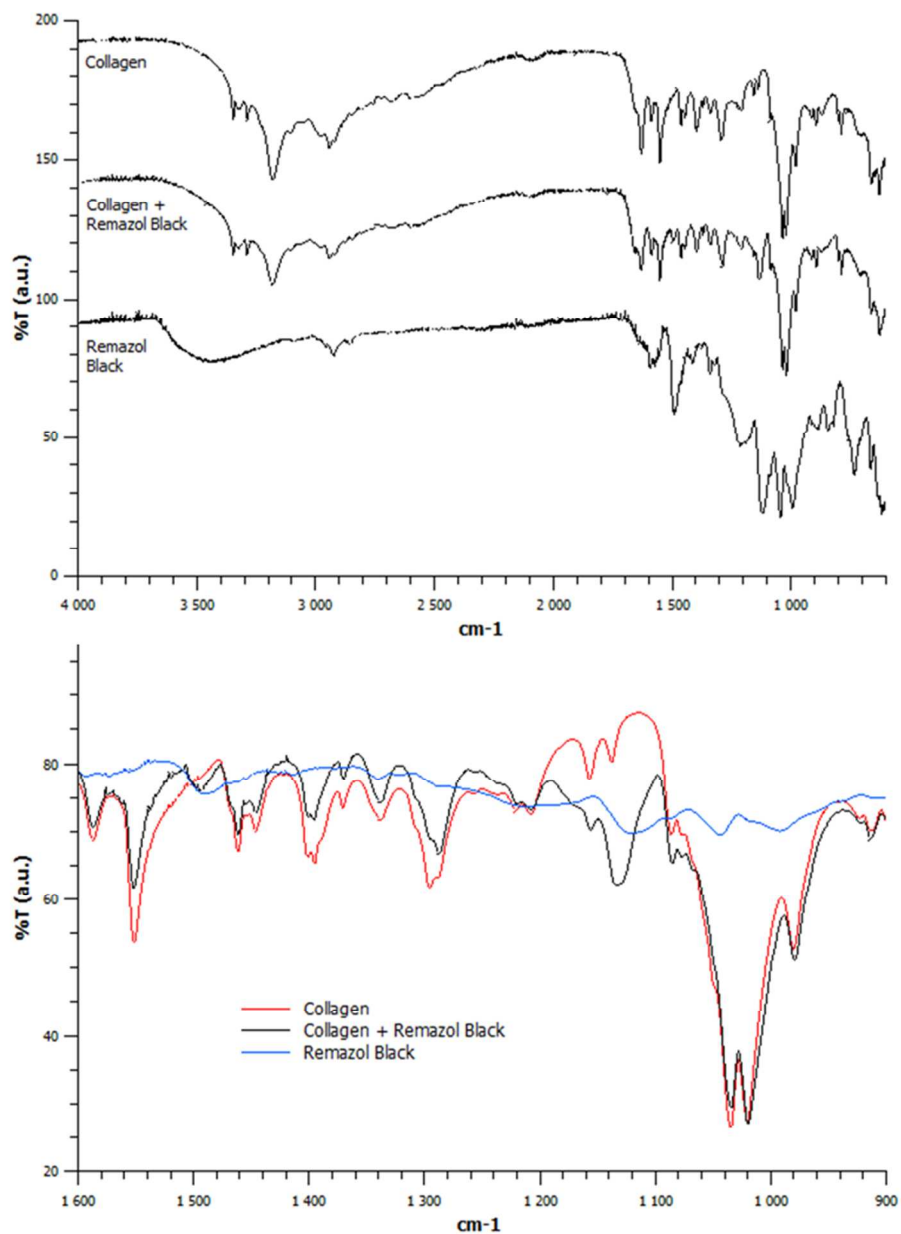
Figure 4: FTIR spectra of collagen hydrogel, Remazol Black and dyed hydrogel in the 4000 and 600 cm^{-1} (upper figure) and higher resolution in the 900 and 1600 cm^{-1} (lower) range.

The impact of RB adsorption at pH 9.00 on the properties of the collagen hydrogels was also investigated by DSC and rheological measurements. As shown in **Figure 5**, the initial

collagen hydrogels have a denaturation temperature, corresponding to the breaking of the protein triple helix, near 55 °C in agreement with the literature. [44] After dye sorption at pH 5.00 there were no significant differences in the thermal stability. Meanwhile there is a slight increase of approximately 4ºC at pH 7.00 and at pH 9.00, the thermal event is shifted to 68 °C. As a comparison, collagen hydrogels cross-linked using malondialdehyde, hexamethylene diisocyanate and glutaraldehyde exhibit 4.2 ºC, 9.0 ºC and 19 ºC increase in the denaturation temperatures. [45]
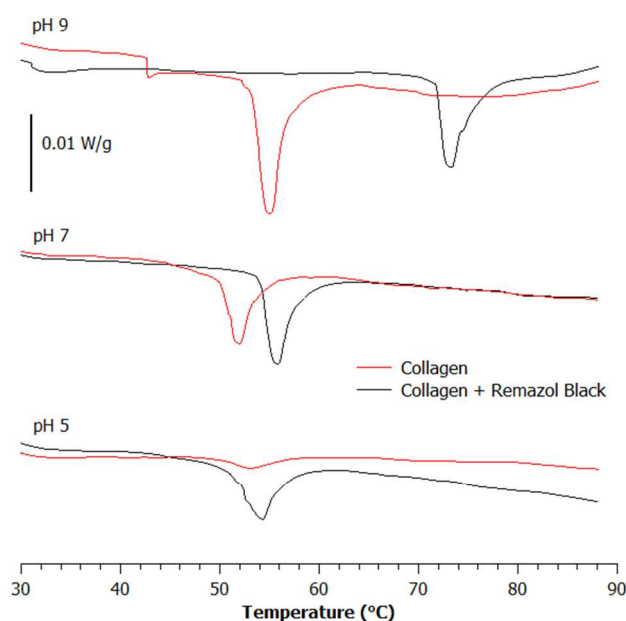
Figure 5: DSC profiles of a control collagen and a Remazol Black dyed sample at various pHs. The samples were first equilibrated at 20 °C before the heating ramp. Exotherms are up.

Pure collagen hydrogels tend to deform under their own weight and are relatively fragile (**Figure 6a**) while dyed collagen gels keep their original shape and are easy to handle (**Figure 6b**). Rheological measurements also indicate a significant stabilization of the

collagen hydrogel upon reaction with RB (**Figure 6c**). The G' modulus at 10 kHz increased

from 0.1 to 1 kPa and G'' from 0.03 to 0.2 Pa. The increase in the values of G' and G'' is

higher than the obtained with concentrated collagen hydrogels, [46] collagen nanocomposites

[46] silicified collagen [47] and even for some glutaraldehyde-fixed collagen hydrogels.[46, 47]
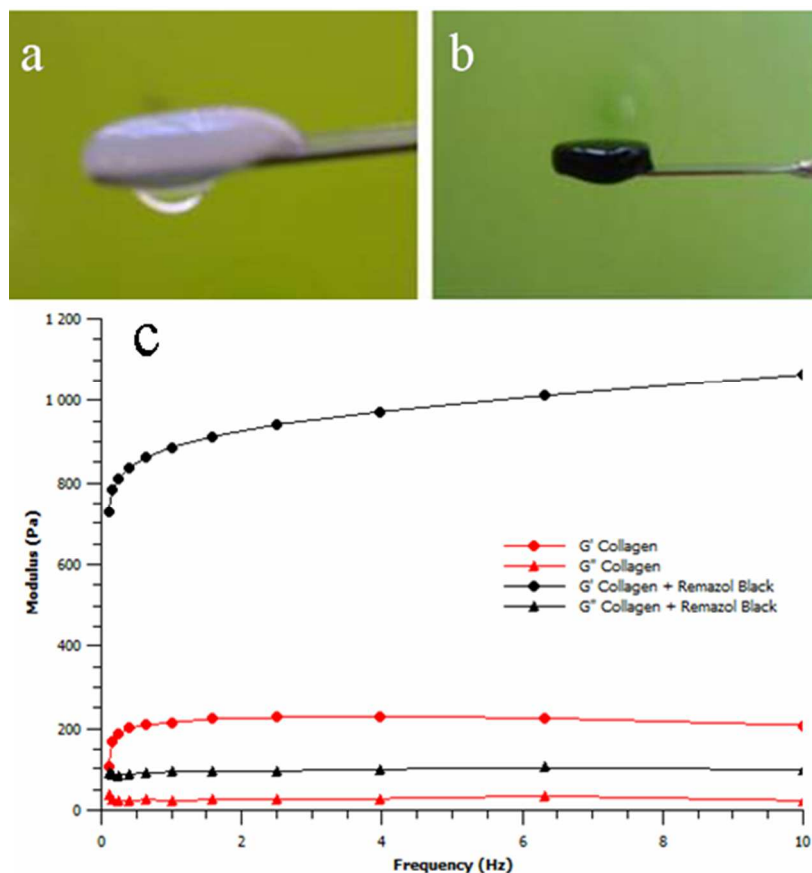
Figure 6: Photograph of (a) collagen hydrogel and (b) dyed collagen; (c) rheological properties of collagen (red lines) and dyed collagen (black lines) hydrogels with the frequency as the variable. Deformation is fixed at 0.1 %.

The hydrogel cross-linking had another interesting consequence on its properties. When weight loss and volume reduction *vs*. time upon drying in ambient conditions were

registered, both dye exposed and not exposed hydrogels showed a rapid weight loss during the first 40 minutes, followed by a continuous slow decrease down to 70 minutes (**Figure 7a**). However, after 70 minutes, the RB-collagen gels exhibited ca. 5% of the initial volume (**Figure 7 b-d**) whereas the pure hydrogel volume was impossible to measure due to its extreme dehydration. This is attributed to the strong contraction of the collagen network upon drying while the crosslinking of the collagen by RB enhance interfibrillar interactions and therefore limits its contraction.[48]
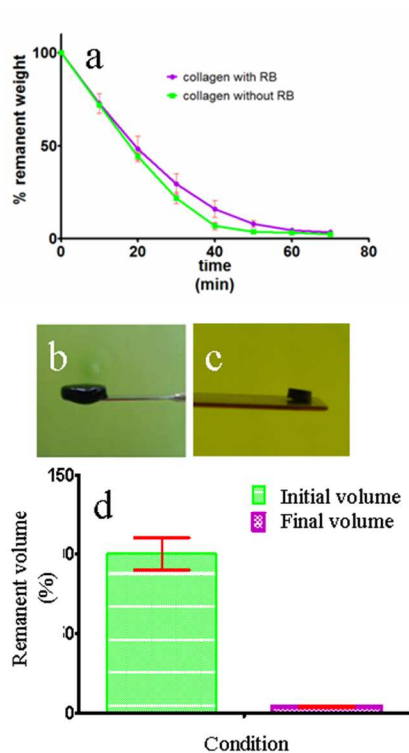
Figure 7: (a) Percentage of weight loss of the gels versus time; representative photographs of dyed collagen (b) before and (c) after 70 min in ambient conditions; (d) percentage of the remaining volume versus time for dyed collagen. (mean ± SD from 10 replicates).

To further understand the mechanisms of interactions between RB and collagen gels, the kinetics of dye sorption were investigated at pH 9.00. The sorption rate varied with the dye concentration but the sorption equilibrium was reached in less than 24 h in all situations (**figure 8**). The results were subjected to kinetic analysis using the pseudo-first-order, pseudo-second-order, Elovich and modified Freundlich models.
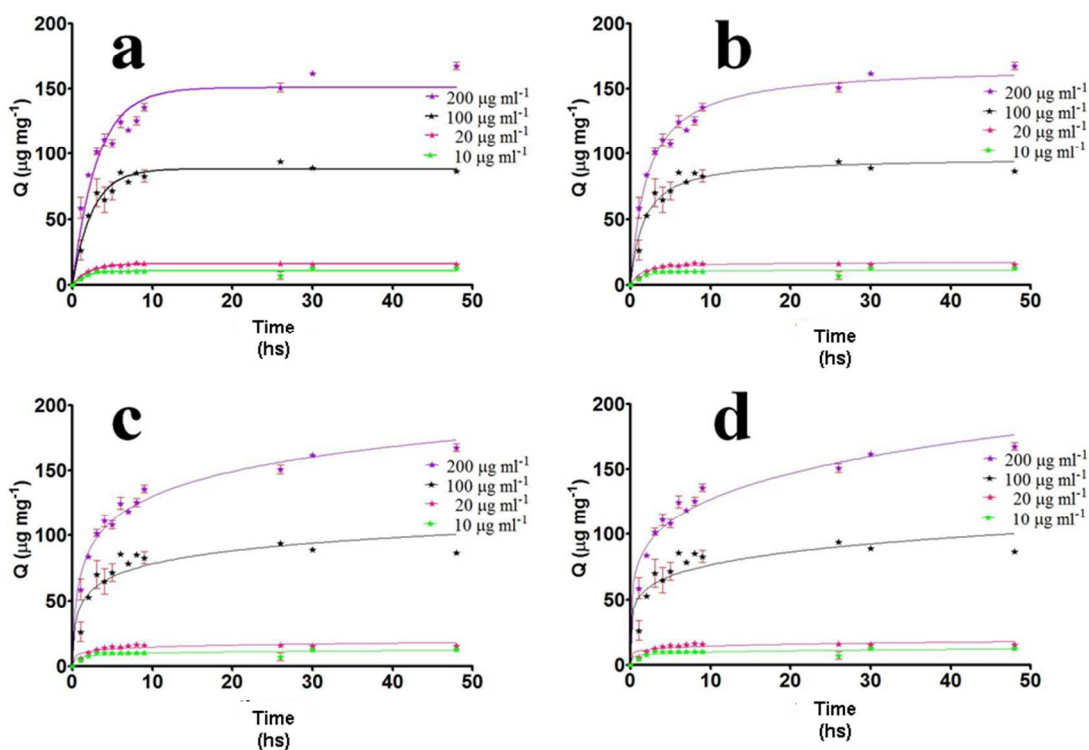
Figure 8: Decoloration kinetics adjusted with the: (a) pseudo first order, (b) pseudo second order, (c) Elovich and (d) modified Freundlich models for RB adsorption onto collagen hydrogels

As can be seen in **Table 1**, no model was satisfactory at the lowest dye concentration (10 $\mu g.mL^{-1}$). This can be attributed to the fact that nearly 100 % of the initial dye content is adsorbed on the collagen network within the very first minutes of the reaction so that a

limited number of experimental points are available. At intermediate concentrations (20 and 100 $\mu g.mL^{-1}$), neither the Elovich nor the modified Freundlich model allows for a suitable fitting of the experimental data ($R^2 < 0.86$). Hence, in these conditions, the sorption process is not mainly based on chemisorption and the dye transport to the collagen surface does not involve intra-particle diffusion. In contrast, both pseudo-first- and pseudo–second-order models provide reasonable fitting of the data. At the highest tested concentration (200 $\mu g.mL^{-1}$), the pseudo-second-order model is the most accurate. Importantly, the Elovich model also provides a suitable fitting of the experimental data. This can be explained considering that the covalent binding of the dye on the collagen surface becomes more significant. Therefore, the kinetic barrier corresponding to the Michael addition reaction at the fiber surface has to be taken into account and the contribution of chemisorption to the overall adsorption process should be considered. One important outcome of these data is that the balance between physisorption and chemisorption mechanisms depends on the dye concentration.

Table 1: Adjustment parameters and constants obtained from the pseudo first order, pseudo second order, Elovich and modified Freundlich kinetic models for RB adsorption onto collagen hydrogels at pH 9.00.

	Pseudo 1° order			Pseudo 2° order			Elovich			Modified Freundlich		
Cc RB	q_e	k_1	R^2	q_e	k_2	R^2	β	α	R^2	k_F	M	R^2
(μg.mL^{-1})	(μg.mg^{-1})	(mg.μg^{-1}.h^{-1})		(μg.mg^{-1})	(mg.μg^{-1}.h^{-1})		(g.μmol^{-1})	(μmol.g^{-1}.h^{-1})		(L.g^{-1}.h^{-1})		
	$\pm$ SD	$\pm$ SD		$\pm$ SD	$\pm$ SD		$\pm$ SD	$\pm$ SD		$\pm$ SD	$\pm$ SD	
200	150.6	0.3206	0.9287	167.1	0.02789	0.9998	0.03658	317.0	0.9771	314.4	4.797	0.9579
	±4.3	±0.03		±3.17	±3x10^{-3}		±2x10^{-3}	±59.91		±11.83	±0.32	
100	88.34	0.4082	0.9401	97.16	0.006177	0.9295	0.06991	341.4	0.8582	206.7	5.834	0.8234
	± 2.4	± 0.04		±3.4	±1x10^{-3}		±0.01	±22.29		±16.80	±1.05	
20	15.92	0.4998	0.9867	17.34	0.04622	0.9295	0.4690	205.3	0.8586	42.50	7.512	0.8302
	±0.17	±0.02		±0.42	±7x10^{-3}		±0.08	±18.93		±2.84	±1.50	
10	10.51	0.6623	0.7714	11.52	0.08676	0.7609	0.7380	224.9	0.7195	29.43	7.689	0.7071
	±0.46	±0.15		±0.68	0.03		±0.20	±36.8		±2.76	±2.2	

This could be further clarified by obtaining adsorption isotherms at different pHs, that confirmed that the maximum adsorption capacity of the collagen hydrogels is larger at pH 9.00 than at pH 5.00 and 7.00 at all concentrations (**Figure 9**). These isotherms were analyzed using the Langmuir, Freundlich, Dubinin-Radushkevich and Temkin adsorption models.
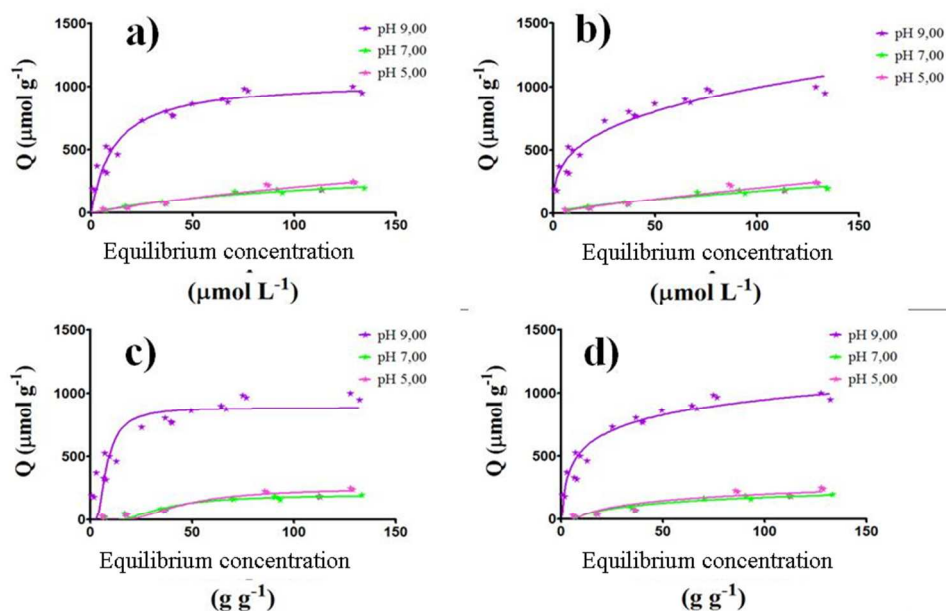
Figure 9: Adsorption isotherms of RB onto collagen at different pHs. The fitting curves were obtained using (a) Langmuir, (b) Freundlich, (c) Dubinin-Radushkevich and (d) Temkin equations

The differences in the fitting parameters found between the Langmuir and Freundlich models were small (**Table 2**). The Langmuir model is based on the assumption that adsorption exists up to the formation of a homogeneous monolayer of the adsorbate interacting with the sorbent. Thus, a tendency to saturate the interaction sites of the hybrid matrices could be deduced from these results. The Freundlich model presents a better adjustment to materials with heterogeneous adsorption sites. Here, the good fitting to this

model further confirms the presence of multiple interactions between the dye and the collagen hydrogel. In addition, the value of n significantly drifts closer to 0 with increasing pH, indicating the increased heterogeneity in terms of interactions of the dye molecule with the collagen surface. [49] Interestingly, the Freundlich model appears to fail at reproducing sorption values at high initial dye concentration at pH 9.00. Coming back to the kinetics studies, it can be suggested that an excess of dyes can lead to the saturation of binding sites by physisorption or electrostatic interactions, which decreases the number of sites available for covalent binding.

The Dubinin-Radushkevich model shows a similar failure in reproducing sorption data for high concentration of dyes at pH 9.00 whereas it allows for a reasonable fitting of the sorption values in more acidic conditions (**Table 2**). The constant related to the adsorption energy (K_{DR}) increases when the pH decreases in agreement with the adsorption phenomena that take place at lower pH and the predominant covalent interaction that occurs at pH 9.00. On the contrary, the Temkin model is more suitable for basic conditions where the parameter related to the heat of sorption (B) is also higher.

The standard free energy (ΔG^0) of the adsorption process can be obtained using the following equation:

$$\Delta G^0 = -RT \ln K_a \qquad (15)$$

with K_a being the equilibrium constant of the Langmuir equation. The value of ΔG^0 for all conditions studied is presented in **Table 2**, where it can be readily concluded that the process is spontaneous. However, ΔG^0 is lower at pH 9.00 which can be due both to the

26

difference in enthalpy and in entropy between electrostatic and covalent binding. In this sense, an increase in enthalpy by tighter covalent binding may directly affect the entropy by the restriction of mobility of the dyed-collagen interacting molecules in agreement with the restriction mobility and increased thermal stability observed by DSC.

The mean free energy value of adsorption E_{DR} (kJ.mol^{-1}) can be calculated using the Dubinin-Radushkevich equation:

$$E_{DR} = (2K_{DR})^{-1/2} \qquad (16)$$

In the adsorption processes, where chemical interactions of weak intensity (such as electrostatic interactions) are dominant, the value of the E_{DR} parameter is between 8-16 kJ.mol^{-1}. Lower values are related to physisorption processes and values higher than 16 kJ.mol^{-1} are related to coordination or covalent bonds formation. [21, 31] Herein, E_{DR} values obtained at pHs 5.00 and 7.00 are around 20 kJ.mol^{-1} suggesting significant interaction between the dye and collagen. At pH 9.00 the E_{DR} value was 42 kJ.mol^{-1}, supporting the hypothesis of stronger covalent bond formation.

Table 2: Fitting parameters and constants obtained from the analysis of the applied isotherm models of RB adsorption onto collagen hydrogels at different pHs.

		Collagen hydrogel pH 9.00		Collagen hydrogel pH 7.00		Collagen hydrogel pH 5.00	
Model	Parameter	Value	R^2	Value	R^2	Value	R^2
Langmuir	q_m (µmol/g)	1052.0	0.9300	383.8	0.9650	709.2	0.9359
	± SD	± 43.1		± 50.0		± 292.2	
	K_a (L/mmol)	11.24		111.40		243.60	
	± SD	± 1.86		± 26.04		± 142.90	
	ΔG^0 (kJ/mol)	-5.990		-11.700		-13.600	
Freundlich	K	2015.0	0.9317	843.8	0.9454	1314.0	0.9297
	± SD	± 158.0		± 121.9		± 292.6	
	N	0.3088		0.6742		0.8119	
	± SD	±0.0251		± 0.0586		± 0.0954	
Dubinin-Radushkevich	q_{DR} (µmol/g)	888.2	0.7680	202.9	0.9150	257.5	0.9197
	± SD	± 41.8		± 9.7		± 14.3	
	K_{DR}(mol^2/kJ^2)	8.70		162.70		255.90	
	± SD	± 1.96		± 30.40		± 48.93	
	E_{DR} (kJ/mol)	42.15		20.14		22.69	
Temkin	K (mL/mg)	177.20	0.9194	65.21	0.9287	75.68	0.8433
	± SD	± 12.36		± 4.38		± 8.43	
	B (J/mol)	2.1160		0.1517		0.1447	
	± SD	± 0.5994		± 0.0213		± 0.0330	

4. Conclusion

The Remazol black dye can act as a cross-linker for type I collagen hydrogels. This results in a significant enhancement of the thermal stability and rheological properties of the protein network. The formation of a covalent bond between collagen and the dye *via* Michael addition reaction is supported by the alkaline pH conditions required for hydrogel stabilization as well as by the values of sorption energies. At neutral and acid pH this reaction does not happen and electrostatic interactions seem to be responsible, at least in part, of the observed sorption process.

These data suggest that type I collagen hydrogels exhibit several advantages for reactive azo-dye remediation from water. Sorption capacity of collagen hydrogel at pH 9.00 was ca. 1 mmol.g^{-1} (*i.e.* 1 g.g^{-1}). Even in acidic conditions that are closer to natural waters, the capacity was > 0.5 g.g^{-1}, larger than reported values for activated carbon.[50, 51] The adsorption process is fast, the adsorbent (collagen) is biodegradable, and azo dyes don't suffer rupture that could origin products even more toxic than the dye without degradation. The interaction between collagen and dye is chemically-stable limiting the risk of secondary contamination due to dye leaching from the sorbent. Another advantage of such hydrogels is their ability to reduce the generation of waste due to their strong reduction in weight and volume upon drying that should reduce the needed storage area leading also to reduction costs. Their application in water remediation would also constitute a new valorization route for industrial processes producing collagen as waste. In parallel cross-linked collagen hydrogels are currently widely used for biomedical applications but they face an important issue related to the cytotoxicity of the cross-linking agent. Relevant biological data for RB are still scarce but suggest that it exhibits a lower toxicity than

glutaraldehyde,[52] calling for a deeper investigation of the in vitro and in vivo properties of these dye-collagen hydrogels.

References

1.   S. Rodríguez Couto, *Biotechnol. Adv.*, 2009, **27**, 227.

2.   R. C. Kuhad, N. Sood, K. K. Tripathi, A. Singh and O. P. Ward, in *Adv. Appl. Microbiol.*, Academic Press, Editon edn., 2004, vol. 56, pp. 185.

3.   H. Ali, *Water Air Soil Pollut*, 2010, **213**, 251.

4.   I. K. Konstantinou and T. A. Albanis, *Appl. Catal. B: Environ.*, 2004, **49**, 1.

5.   H. M. Pinheiro, E. Touraud and O. Thomas, *Dyes Pigments*, 2004, **61**, 121.

6.   B. C. Ventura-Camargo and M. A. Marin-Morales, *Text. Light Ind. Sci. Technol.*, 2013, **2**, 85.

7.   M. A. Brown and S. C. De Vito, *Critical Rev. Environ. Sci. Technol.*, 1993, **23**, 249.

8.   E. Forgacs, T. Cserháti and G. Oros, *Environ. Inter.*, 2004, **30**, 953.

9.   N. R. Rane, V. V. Chandanshive, R. V. Khandare, A. R. Gholave, S. R. Yadav and S. P. Govindwar, *RSC Advances*, 2014, **4**, 36623.

10.   A. Ahmad, S. H. Mohd-Setapar, C. S. Chuong, A. Khatoon, W. A. Wani, R. Kumar and M. Rafatullah, *RSC Advances*, 2015, **5**, 30801.

11.   S. Dong, J. Feng, M. Fan, Y. Pi, L. Hu, X. Han, M. Liu, J. Sun and J. Sun, *RSC Advances*, 2015, **5**, 14610.

12.   Y. Huang, J. Li, X. Chen and X. Wang, *RSC Advances*, 2014, **4**, 62160.

13.   R. K. Upadhyay, N. Soin and S. S. Roy, *RSC Advances*, 2014, **4**, 3823.

14.   M. V. Tuttolomondo, G. S. Alvarez, M. F. Desimone and L. E. Diaz, *J. Environ. Chem. Eng.*, 2014, **2**, 131.

15.   A. Walcarius and L. Mercier, *J. Mater. Chem.*, 2010, **20**, 4478.

16.   A. S. Bhatt, P. L. Sakaria, M. Vasudevan, R. R. Pawar, N. Sudheesh, H. C. Bajaj and H. M. Mody, *RSC Advances*, 2012, **2**, 8663.

17.   A. Pourjavadi, M. Nazari and S. H. Hosseini, *RSC Advances*, 2015, **5**, 32263.

18.   Y. Wu, M. Zhang, H. Zhao, S. Yang and A. Arkin, *RSC Advances*, 2014, **4**, 61256.

19.   D. Parasuraman and M. J. Serpe, *ACS Appl. Mater. Interf.*, 2011, **3**, 2732.

20.   J. H. Bowes and R. H. Kenten, *Biochem. J.*, 1948, **43**, 358.

21.   P. Bornstein and H. Sage, *Ann. Rev. Biochem.*, 1980, **49**, 957.

22.   R. W. Glanville, D. Breitkreutz, M. Meitinger and P. P. Fietzek, *Biochem. J.*, 1983, **215**, 183.

23.   K. A. Piez, E. A. Eigner and M. S. Lewis, *Biochem.*, 1963, **2**, 58.

24.   J. E. Eastoe, *Biochem. J.*, 1955, **61**, 589.

25.   Z. Zhang, G. Li and B. SHI, *J. Soc. Leather Technol. Chem.*, 2006, **90**, 23.

26.   R. L. Trelstad, V. M. Catanese and D. F. Rubin, *Anal. Biochem.*, 1976, **71**, 114.

27.   J. Einbinder and M. Schubert, *J. Biol. Chem.*, 1951, **188**, 335.

28.   E. Mocan, O. Tagadiuc and V. Nacu, *Curierul medical*, 2011, **2**, 3.

29.   I. Bergman and R. Loxley, *Anal. Chem.*, 1963, **35**, 1961.

30.   D. Agarwal, K. Sen and M. L. Gulrajani, *J. Soc. Dye. Colour.*, 1997, **113**, 174.

31.   S. Kuo and E. G. Lotse, *Proc. Soil Sci. Soc. Am.* , 1973, 50.

32.   D. Kumar, L. K. Pandey and J. P. Gaur, *Coll. Surf B: Biointer.*, 2010, **81**, 476.

33.   A. M. El-Kamash, A. A. Zaki and M. A. El Geleel, *J. Hazard. Mater.*, 2005, **127**, 211.

34.   A. O. Dada, A. P. Olalekan, A. M. Olatunya and O. Dada, *J. Appl. Chem.*, 2012, **3**, 38.

35.   S. W. Won, M. H. Han and Y.-S. Yun, *Water Res.*, 2008, **42**, 4847.

36.   G. S. Alvarez, C. Hélary, A. M. Mebert, X. Wang, T. Coradin and M. F. Desimone, *J. Mater. Chem. B*, 2014, **2**, 4660.

37.   D. C. P. Trut, ed., *Reactive dyes for textile fibers*, Society of Dyers and Colourists, 1999.

38.   K. Uddin and S. Hossain, *Inter. J. Eng. Technol.*, 2010, **10**, 22.

39.   A. A. Haroun, *Dyes Pigments*, 2005, **67** 215.

40.   A. Kantouch, O. Allam, L. El-Gabry and H. El-Sayed, *Indian J. Fibre Textile Res.*, 2011, **37**, 157.

41.   H. Jung Cho and D. M. Lewis, *Color. Technol.*, 2002, **118**, 198.

42.   A. Mandal, S. Sekar, N. Chandrasekaran, A. Mukherjee and T. P. Sastry, *J. Mater. Chem. B*, 2015, **3**, 3032.

43.   M. P. Shah, *Inter. J. Environ. Biorem. Biodeg.*, 2014, **2**, 139.

44.   S. Heinemann, T. Coradin and M. F. Desimone, *Biomater. Sci.*, 2013, **1**, 688.

45.   C. A. Miles, N. C. Avery, V. V. Rodin and A. J. Bailey, *J. Mol. Biol.*, 2005, **346**, 551.

46.   M. F. Desimone, C. Hélary, I. B. Rietveld, I. Bataille, G. Mosser, M. M. Giraud-Guille, J. Livage and T. Coradin, *Acta Biomater.*, 2010, **6**, 3998.

47.   M. F. Desimone, C. Hélary, S. Quignard, I. B. Rietveld, I. Bataille, G. J. Copello, G. Mosser, M. M. Giraud-Guille, J. Livage, A. Meddahi-Pellé and T. Coradin, *ACS Appl. Mater. Interf.*, 2011, **3**, 3831.

48.   P. L. Chandran, D. C. Paik and J. W. Holmes, *Connective Tissue Res.*, 2012, **53**, 10.3109/03008207.2011.640760.

49.   K. Y. Foo and B. H. Hameed, *Chem. Eng. J.*, 2010, **156**, 2.

50.   N. F. Cardoso, R. B. Pinto, E. C. Lima, T. Calvete, C. V. Amavisca, B. Royer, M. L. Cunha, T. H. M. Fernandes and I. S. Pinto, *Desalination*, 2011, **269**, 92.

51. L. Donnaperna, L. Duclaux, R. Gadiou, M. P. Hirn, C. Merli and L. Pietrelli, *J. Coll. Interf. Sci.*, 2009, **339**, 275.

52. C. Wang, A. Yediler, D. Lienert, Z. Wang and A. Kettrup, *Chemosphere*, 2003, **52**, 1225.